



RAPID COMMUNICATION

SUV39H1-driven NFATc1 methylation is essential for the c-Cbl-mediated degradation of NFATc1 in an osteoclast lineage



Bone undergoes continuous remodeling by tightly-coordinated actions of bone-resorbing osteoclasts and bone-forming osteoblasts.¹ Recent studies document that the dysregulation of histone methylation profiles is associated with the progression of osteoclastogenesis. However, the specific epigenetic modifiers are incompletely understood. In this study, we demonstrate an inhibitory role of a variation 3–9 homolog 1 (SUV39H1) in osteoclast formation. Public datasets find that mRNA levels of several methyltransferases are gradually decreased during osteoclastogenesis. Among them, a decrease in SUV39H1 mRNA level leads to accelerated osteoclast differentiation with the induction of several osteoclastogenic genes both *in vivo* and *in vitro*. In this regard, SUV39H1 directly binds and methylates a nuclear factor of activated T cells 1 (NFATc1) at lysine 267 of the regulatory domain (RD) motif. Of note, SUV39H1 enhances c-Cbl-dependent NFATc1 ubiquitination. Reduced NFATc1 methylation by the knockdown of SUV39H1 significantly decreases c-Cbl-dependent NFATc1 ubiquitination. Finally, SUV39H1 methylates lysine 9 of histone 3 (H3K9) at osteoclastogenic gene promoters, thereby repressing NFATc1 transcriptional activity. Taken together, our findings reveal that SUV39H1 plays both epigenetic and enzymatic roles in its action as an intrinsic suppressor of osteoclastogenesis.

The involvement of lysine methyltransferases (KMTs) during osteoclastogenesis was explored by examining the mRNA levels of KMTs using bone marrow-derived macrophages (BMMs) in the public database (GSE57468). When the samples were divided into the NFATc1_{high} and NFATc1_{low} expressing groups, the gene set enrichment analysis (GSEA) showed that KMT activity was negatively correlated with NFATc1 expression (Fig. S1A). Next, we divided KMTs into two groups (histone/non-histone methylases and histone methylases) and analyzed the mRNA levels of specific KMTs,

which showed that some KMTs from the public dataset were not consistently decreased during osteoclastogenesis (Fig. S1B). We then verified the decreasing tendency of KMTs using an *in vitro* culture system. Among histone and non-histone KMTs, only *Ehmt2* and *Suv39H1* mRNA levels were decreased in receptor activation of nuclear factor κB ligand (RANKL)-treated cells. Among the histone KMTs, *Rbbp5* and *Wdr5* showed decreasing trends during osteoclastogenesis (Fig. S1C). To characterize the roles of these enzymes, osteoclastogenesis upon RANKL stimulation was assessed using tartrate-resistant acid phosphatase (TRAP) staining. Only SUV39H1 knockdown significantly reinforced RANKL-induced osteoclastogenesis in BMMs and RAW 264.7 cells (Fig. S1D–E). Consistent with the decrease in its mRNA level, the expression of SUV39H1 was reduced by RANKL treatment (Fig. S1F). These results led us to investigate the inhibitory function of SUV39H1 in osteoclastogenesis.

Because NFATc1 is a major transcription factor that mediates the expression of many genes essential to osteoclast differentiation,² we tested NFATc1 protein level and transcriptional activity. The resulting loss of SUV39H1 using si-RNAs increased multi-nuclear TRAP-positive osteoclasts in both BMMs and RAW 264.7 cells (Fig. 1A; Fig. S2A). SUV39H1 depletion induced NFATc1 expression in both cells during osteoclastogenesis (Fig. S2B). The silencing of SUV39H1 significantly enhanced the mRNA levels of osteoclastogenic genes such as *Nfatc1*, *Trap*, *Oscar*, and *Ctsk* during osteoclastogenesis (Fig. S2C). Taken together, these results show that SUV39H1 impairs osteoclastogenesis by regulating NFATc1 expression and its downstream genes.

The role of SUV39H1 in bone resorption was studied in a mouse model. PBS- or RANKL-soaked collagen sponges containing si-RNAs/jetPEI (transfection reagents) were implanted on the calvariae of mice (Fig. S3A). Ten days after implantation, the calvariae were decalcified for micro-CT scanning and TRAP staining. Those results and measurements of the total porosity and TRAP staining area

Peer review under responsibility of Chongqing Medical University.

<https://doi.org/10.1016/j.gendis.2023.06.008>

2352-3042/© 2023 The Authors. Publishing services by Elsevier B.V. on behalf of KeAi Communications Co., Ltd. This is an open access article under the CC BY-NC-ND license (<http://creativecommons.org/licenses/by-nc-nd/4.0/>).

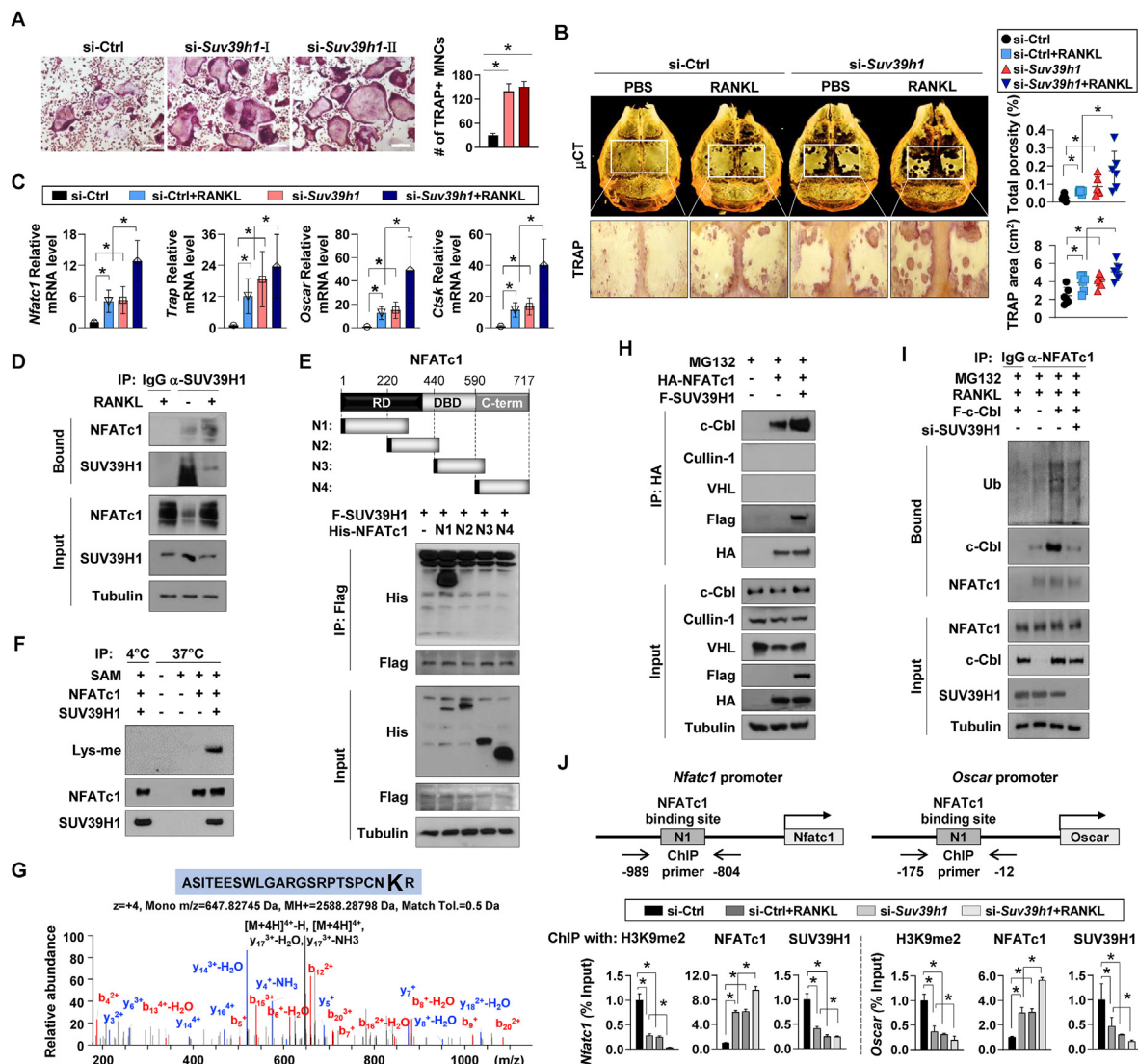


Figure 1 The importance of SUV39H1 as an intrinsic suppressor of osteoclastogenesis. **(A)** Bone marrow-derived macrophages (BMMs) transfected with si-Suv39h1 were treated with RANKL for 3 days. Differentiated osteoclasts were visualized using TRAP staining (left) and the number of TRAP-positive multinucleated cells was quantified (right). Mean \pm SD ($n = 3$). $*P < 0.05$. MNCs, multi-nuclear cells. Scale bar, 200 μ m. **(B, C)** Mice calvariae were implanted with collagen sponges soaked in PBS or RANKL. si-ctrl or si-Suv39h1 were injected into the calvariae twice during 10 days, at 5-day intervals ($n = 6$). Micro-CT and TRAP staining images of mice calvariae with si-RNAs/jetPEI and RANKL on day 10 after implantation were shown. Total porosity (%) and TRAP staining area (cm^2) in the calvariae were evaluated with micro-CT. Total RNAs were harvested from the calvariae, and mRNA expression was evaluated using RT-qPCR. Gene expression levels were quantified relative to 18S mRNA. Mean \pm SD ($n = 3$). $*P < 0.05$. **(D)** RAW 264.7 cells were treated with RANKL for 16 h, incubated with anti-SUV39H1 antibody at 4 $^{\circ}\text{C}$ for 16 h, and the immunoprecipitates were then subjected to Western blotting. **(E)** Schematic diagram of the four segments of the NFATc1 gene (upper panel). 293T cells were co-transfected with the indicated fragments (lower panel). Proteins were pulled down using Flag affinity beads and analyzed using Western blotting. **(F)** *In vitro* methylation assay was performed. Recombinant NFATc1 protein was reacted with purified SUV39H1 using a Flag affinity gel in methylation buffer. Methylated NFATc1 was detected using an anti-methylated lysine antibody. **(G)** Methylation sites within the RD motif were identified by mass spectrometry. Peptide identification was based on molecular ions. The detected y and b fragments were indicated in the sequence. The mass spectrum of the lysine methylation peptide ASI-TEESWLGLGARGSRPTSPCNKR was shown. **(H)** 293T cells were transfected with the indicated plasmids and treated with MG132 (10 μM) for 8 h. Cell lysates were immunoprecipitated with HA beads and then subjected to Western blotting. **(I)** Cells were co-transfected with the indicated plasmids. Proteins were pulled down using an anti-NFATc1 antibody and then separated by SDS-PAGE. **(J)** Lysates were prepared from BMMs transfected with the si-RNAs and stimulated with RANKL for one day. The lysates were used in chromatin immunoprecipitation assay for H3K9me2, NFATc1, and SUV39H1 at the *Nfatc1* and *Oscar* promoters. Mean \pm SD ($n = 3$). $*P < 0.05$.

showed more significant bone resorption in the RANKL-treated or si-*Suv39h1*-treated calvariae than in the PBS-treated calvariae. Moreover, synergistic bone resorption was seen in the latter (Fig. 1B; Fig. S3B, C). The mRNA levels of NFATc1-driven genes were elevated by si-*Suv39h1* on the mice calvariae, both in the presence and absence of RANKL (Fig. 1C). These results suggest that SUV39H1 is a negative regulator of osteoclastogenesis *in vivo*.

Because SUV39H1 methylates both histone and non-histone proteins,^{3,4} we hypothesized SUV39H1 methylates and subsequently regulates NFATc1 protein. Immunoprecipitation assay evidenced the direct binding of SUV39H1 to endogenous or ectopically expressed NFATc1 (Fig. 1D; Fig. S4A). To identify the binding domain of NFATc1 involved in complex formation with SUV39H1, we generated four segments of NFATc1 (N1–N4) and found a decrease and interaction only in the RD domain (N1) (Fig. 1E; Fig. S4B). We then investigated the methylation of NFATc1 by SUV39H1. The levels of endogenous NFATc1 and its RD motif were reduced, whereas lysyl methylation of both proteins increased in response to the ectopic expression of SUV39H1. In contrast, SUV39H1 knockdown in RAW264.7 cells decreased NFATc1 methylation (Fig. S4C–E). NFATc1 methylation by SUV39H1 was confirmed in an *in vitro* methylation assay using purified SUV39H1 and NFATc1 proteins (Fig. 1F).

The sites of NFATc1 methylation by SUV39H1 were investigated in an LC-MS/MS analysis of immunoprecipitates obtained with anti-His antibody in cells transfected with Flag-SUV39H1 or si-SUV39H1. LC-MS/MS showed that lysines 215 and 267 (K215 and K267) and arginines 204, 220, and 234 in the RD motif were methylated. Only K267 methylation disappeared following SUV39H1 knockdown, thus identifying K267 as a specific site of NFATc1 methylation by SUV39H1 (Fig. 1G; Fig. S5A). Moreover, K267 of NFATc1 is evolutionarily conserved across different species (Fig. S5B).

Since methylation modifies the stability of target proteins,⁵ we examined whether the SUV39H1-dependent methylation of NFATc1 affected its stability. The ectopic expression of SUV39H1 reduced ectopic NFATc1 expression (Fig. S6A). The addition of the proteasomal inhibitor MG132 led to the recovery of NFATc1 expression (Fig. S6B) and counteracted the SUV39H1-mediated loss of RD motif (Fig. S6C). Next, whether SUV39H1-mediated methylation is responsible for the proteasomal degradation of NFATc1 was examined. Indeed, SUV39H1 significantly increased the polyubiquitination of full-length NFATc1 and its RD domain (Fig. S6D–E). An analysis of the half-life of NFATc1 using cycloheximide, an inhibitor of protein synthesis, showed a 2.2-fold decrease in the ectopic expression of SUV39H1 (Fig. S6F). Next, we tested SUV39H1 recruits the E3 ubiquitin ligase to NFATc1 for its ubiquitination. Although c-Cbl, Cullin-1, and von Hippel-Lindau tumor suppressor (VHL) have been identified as ubiquitin E3 ligases of NFATc1, we found that only c-Cbl was bound to NFATc1. Of note, the ectopic expression of SUV39H1 reinforced the interaction between NFATc1 and c-Cbl (Fig. 1H), which was impaired when SUV39H1 was knocked down and accompanied by a decrease in c-Cbl-mediated NFATc1 ubiquitination (Fig. 1I). Taken together, these results suggest that SUV39H1-mediated NFATc1 methylation is required for c-Cbl-dependent NFATc1 degradation.

Since SUV39H1 was first identified as an H3K9 methylase, the methylation status of H3 was examined. SUV39H1 knockdown decreased H3K9me2 but induced NFATc1 expression in BMMs and RAW 264.7 cells (Fig. S7A). The role of SUV39H1 as an epigenetic regulator was investigated using chromatin immunoprecipitation. Reduction in H3K9me2 levels was found at the promoters of NFATc1 target genes after RANKL stimulation, together with a further decrease of H3K9me2 in si-*Suv39h1*-transfected cells. In addition, the recruitment of SUV39H1 to the *Nfatc1* and *Oscar* promoters was negatively associated with the abundant recruitment of NFATc1 (Fig. 1J; Fig. S7B).

In conclusion, the findings show that SUV39H1 directly methylates NFATc1, and NFATc1 methylation is essential for subsequent c-Cbl-mediated ubiquitination (Fig. S8). Because SUV39H1 is an epigenetic regulator through its action targeting H3K9 at the promoters of osteoclastogenic genes, we were able to demonstrate that SUV39H1 acts as a molecular suppressor in osteoclastogenesis. Given the important role of SUV39H1 in bone remodeling, this study merits exploration as a therapeutic target in the treatment of bone disorders.

Author contributions

Methodology: D.W.J., H.J.K., H.J., and Y.S.C.; Acquisition of data: D.W.J., H.J.K., S.L., and H.J.; Analysis of data: D.W.J., H.J.K., H.J., E.C.Y., and Y.S.C.; Resources: J.W.P., E.C.Y., N.K., and Y.S.C.; Writing-original draft: D.W.J., and Y.S.C.; Supervision: Y.S.C. All authors have read and concurred with the content of the manuscript.

Conflict of interests

The authors declare that they have no competing interests.

Funding

This work was supported by the National Research Foundation of Korea (No. 2019R1A2C2083886, 2018R1A5A20-25964) and supported by the Cooperative Research Program of Basic Medical Science and Clinical Science from Seoul National University College of Medicine (No. 800-20220312).

Data availability

The data used to support the findings of this study are available from the corresponding authors upon request.

Acknowledgements

D.W.J. and S.L. received a scholarship from the BK21-plus program of the Republic of Korea.

Appendix A. Supplementary data

Supplementary data to this article can be found online at <https://doi.org/10.1016/j.gendis.2023.06.008>.

References

1. Chen X, Wang Z, Duan N, Zhu G, Schwarz EM, Xie C. Osteoblast-osteoclast interactions. *Connect Tissue Res.* 2018;59(2):99–107.
2. Lorenzo J, Horowitz M, Choi Y. Osteoimmunology: interactions of the bone and immune system. *Endocr Rev.* 2008;29(4):403–440.
3. Kim HJ, Park JW, Lee KH, et al. Plant homeodomain finger protein 2 promotes bone formation by demethylating and activating Runx2 for osteoblast differentiation. *Cell Res.* 2014;24(10):1231–1249.
4. Yaseen I, Choudhury M, Sritharan M, Khosla S. Histone methyltransferase SUV39H1 participates in host defense by methylating mycobacterial histone-like protein HupB. *EMBO J.* 2018;37(2):183–200.
5. Lee JM, Lee JS, Kim H, et al. EZH2 generates a methyl degron that is recognized by the DCAF1/DDB1/CUL4 E3 ubiquitin ligase complex. *Mol Cell.* 2012;48(4):572–586.

Do-Won Jeong^{a,b,1}, Hye-Jin Kim^{a,b,1}, Jong-Wan Park^{a,c},
Seulbee Lee^{a,b}, Hyeryeon Jung^d, Eugene C. Yi^d,
Nacksung Kim^e, Yang-Sook Chun^{a,b,c,*}

^aDepartment of Biomedical Sciences, Seoul National University College of Medicine, Seoul 03080, Republic of Korea

^bDepartment of Physiology, Seoul National University College of Medicine, Seoul 03080, Republic of Korea
^cIschemic/Hypoxic Disease Institute, Seoul National University College of Medicine, Seoul 03080, Republic of Korea

^dDepartment of Molecular Medicine and Biopharmaceutical Sciences, Graduate School of Convergence Science and Technology and College of Medicine Or College of Pharmacy, Seoul National University, Seoul 03080, Republic of Korea

^eDepartment of Pharmacology, Chonnam National University Medical School, Gwangju 61469, Republic of Korea

*Corresponding author. Department of Biomedical Sciences Seoul National University College of Medicine, 103 Daehak-ro, Jongno-gu, Seoul 03080, Republic of Korea.
E-mail address: chunys@snu.ac.kr (Y.-S. Chun)

4 August 2022
Available online 14 July 2023

¹ These authors contributed equally to this work.